MATEC Web of Conferences **13**, 04021 (2014)
DOI: 10.1051/matecconf/ 20141304021

Effective Duration of Gas Nitriding Process on AISI 316L for the Formation of a Desired Thickness of Surface Nitrided Layer

Hassan R. S. Mahmoud[1a]*, Syafiq A. Yusoff[1], Azman Zainuddin[1], Patthi Hussain[2], Mokhtar Ismail[2], and Kamal Abidin[1]

[1]Department of Mechanical Engineering, University Technology PETRONAS, Malaysia
[2]Center for Corrosion Research, University Technology PETRONAS, Malaysia

Abstract. High temperature gas nitriding performed on AISI 316L at the temperature of 1200°C. The microstructure of treated AISI 316L samples were observed to identify the formation of the microstructure of nitrided surface layer. The grain size of austenite tends to be enlarged when the nitriding time increases, but the austenite single phase structure is maintained even after the long-time solution nitriding. Using microhardness testing, the hardness values drop to the center of the samples. The increase in surface hardness is due to the high nitrogen concentration at or near the surface. At 245HV, the graph of the effective duration of nitriding process was plotted to achieve the maximum depth of nitrogen diffuse under the surface. Using Sigma Plot software best fit lines of the experimental result found and plotted to find out effective duration of nitriding equation as $Y=1.9491(1-0.7947^{x})$, where Y is the thickness of nitrided layer below the surface and X is duration of nitriding process. Based on this equation, the duration of gas nitriding process can be estimated to produce desired thickness of nitrided layer.

1 Introduction

AISI 316L has a minimum content of 12% chromium, making it highly resistant to corrosion and oxidation [1, 2]. Austenitic stainless steel (ASS) has face-cantered cubic (FCC) [3]. The major drawback in the properties of AISI 316L is its low wear resistance and surface hardness. Low hardness of the surface could lead to the failure of the operational parts and to the operational equipment. Therefore, one of the approaches to improve surface hardness and wear resistance of the steel is by nitriding treatment where its offer the benefits of high dimensional stability, in gas nitriding, the alloy, held at a suitable temperature and bombarded by a nitrogenous gas like ammonia [4]. Nitriding produces the hardest case, no heat treatment is required and corrosion resistance of nitrided parts is maintained [7, 10]. The hardness increased with the increase of nitriding time is due to high nitrogen content in the layer [8]. Maximum value of hardness obtained at the surface and then it gradually decreased to core value. However it still has a small increment of hardness up to 800 μm in depth [9]. This observation evidences that some nitrogen atoms were able to interstitially diffuse to that depth. In industrial practice, a model that predicts the nitriding depth from nitriding conditions and steel composition is useful, because with such a model optimum nitriding conditions for a given steel type could be calculated instead of inferred from a trial and error approach [11]. The sudden

[a] hassanrsmahmoud@gmail.com

drop of the nitrogen content is additional evidence for the occurrence of a new phase. The decrease of nitrogen inside the layer is due to a gradient of interstitially dissolved nitrogen within the modified layer [13]. Due to the lack of information on the effective duration of gas nitriding process of AISI 316L, the objective of this paper is to determine the effective nitriding time in order to get a desired thickness of nitrided surface layer.

2 Experimental set up

The materials received in form of the square bar, with composition of 0.02% C, 0.42% Si, 1.7% Mn, 0.03% P, 0.002% S, 17.19% Cr, 2.06% Mo, 11.54% Ni, 0.31% Co and balance Fe. Using abrasive cutter, AISI 316L was cut by to a dimension of 12.9 mm X 12.9 mm X 6.0 mm. Before the nitriding process was done, the samples were ground and polished, in order to produce a good surface finish. The high temperature gas nitriding process on AISI 316L austenitic stainless steel at the temperature of 1200°C with pressure of 100 mmHg and gas mixture of 500 cm^3/min of N_2 and 500 cm^3/min of NH_3 for different duration of times which are 2, 4, 8 and 24 hours.

The samples were etched with Marble's solution for 30 seconds and washed with acetone and then observed by optical microscope. The Vickers hardness test was carried out to measure the microhardness of both the as- received and nitrided specimens by using 50g load. The data recorded and the graph of hardness vs. depth of nitrided layer was plotted. Sigma Plot software was also used to derive the equation of effective duration of nitriding processes, by performing the curve fitting.

3 Result and discussion

3.1 Metallographic Analysis

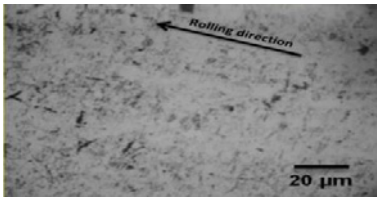

Figure 1: The microstructure of as-received sample

Figure 1 shows a microstructure of as-received sample of AISI 316L. The deformed structure shown indicates that it has been cold work below the recrystallization temperature by the processes such as rolling [16]. The microstructures of the nitrided AISI 316L are shown in Figure 2. The twin's formations were observed in the microstructure of the austenitic stainless steel. The formation of twinning are in multiple slip systems especially in low stacking fault energy (SFE) of the FCC AISI 316L [18]. Twinning is generally considered as a deformation mechanism for the low SFE metals such as ASS or TWIP steel. Grains without mechanical deformation twins contain a high density of planar dislocation structures [17]. The shape of twins in 316L SS is divided into two patterns: suspended twin and transgranular twin [18]. It was observed that the suspended twins consist of four parts: two sides are the coherent twin planes, the head is the incoherent twin plane and the end is grain boundary, which stops in original austenite grain after growth of a section as seen in Figure.2b. Figure 2c shows the morphology of the transgranular twin which consists of four parts: two sides are the coherent twin planes and two ends are the grain boundary. On heating steel through its critical range, transformation to austenite takes place. The austenite grains are extremely small when first formed, but grow in size as the time and temperature are increased. Grain size can be measured using an optical microscope on a transverse metallographic mount, because rolling elongates the grains [19].

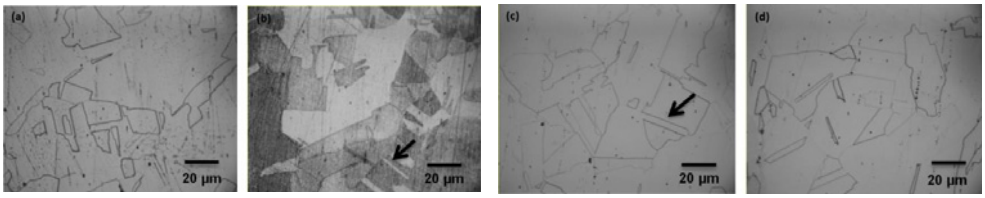

Figure 2: Microstructures of nitrided AISI 316L at **(a)** 2 hours **(b)** 4 hours **(c)** 8 hours **(d) 24** hours

3.2 Microhardness of AISI 316L

From Figure 3, the hardness decreases gradually as the depth increases until reaching values similar to those of the original material. Nitrogen has a strong solid solution hardening effect [20]. Both hardness and nitrogen content decreased monotonically with the distance from the surface. The high nitrogen contents, ∼0.5–1.0 wt. %, are dissolved in austenite, in the 1273–1473K temperature range, in which intense chromium nitride precipitation occurs, greatly increasing the hardness, but impairing the corrosion resistance of stainless steels [21].

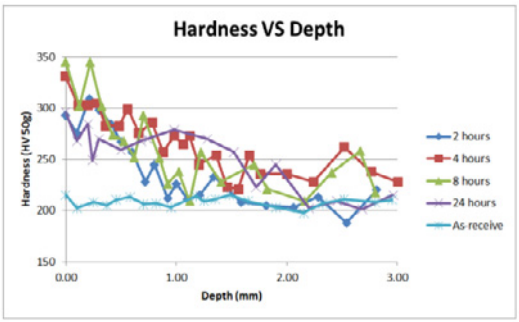

Figure 3: The graph of Hardness vs. Depth

The hardness values drop toward the centre of the specimen. Based on Fader et al. [22], the increase in hardness in the surface layers is due to a larger concentration of nitrogen present in such regions, a larger grain size, and the presence of transformed phase (t'-phase) [22].

3.3 Curve Fitting

The hardness value of specimen with different durations of gas nitriding process is selected to plot the graph. At the hardness value of 245HV; the curve fitting is done by using the Sigma Plot Software. The data of the experimental result is tabulated and the graph of depth versus nitriding time is plotted as shown in Figure 4.

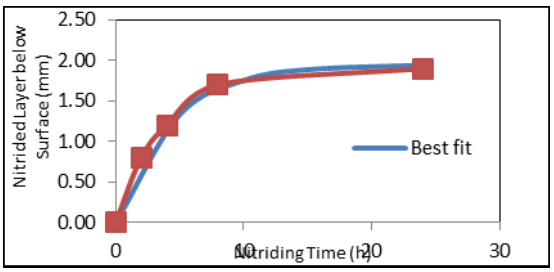

Figure 4: Depth Vs. Nitriding Time

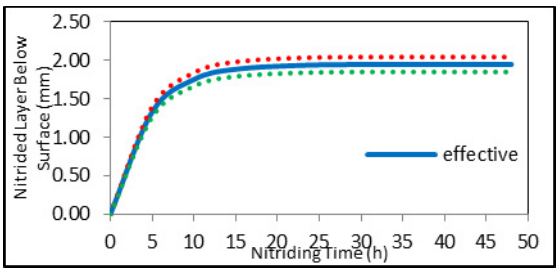

Figure 5: Graph of effective duration of nitriding

Table 1: Experimental result at hardness value 245HV

Nitriding Time (hours)	Nitrided layer (mm)
0	0
2	0.8
4	1.2
8	1.7
24	1.9

Table 2: Result of Curve fitting using Sigma Plot

R	R^2	Adj. R^2	Standard Error of Estimate		
0.9853	0.9709	0.9636	0.1512		
Corrected for the Mean of the observation					
	DF	SS	MS	F	P
Regression	1	3.0499	3.0499	133.4705	0.0003
Residual	4	0.0914	0.0229	--------	--------
Total	5	3.1413	0.6283	--------	--------

The result obtained by the curve-fitting software is tabulated as shown in the Table 2. The 'R' value above is referred to the strength of the linear association between two variables is quantified by the correlation coefficient which is 0.9853. The R^2 is the square of the correlation coefficient, the value R^2 quantifies goodness of fit. It is computed as the fraction of the total variation of the Y values of data points that is attributable to the assumed model curve, and its values typically range from 0 to 1. The R^2 for this curve fitting is 0.9709 which is the values close to 1 indicate a good fit. The adjusted R-squared is a modified version of R-squared that has been adjusted for the number of predictors in the model. The adjusted R-square is 0.9636 which is decrease compare to the R-square. The adjusted R-squared increases only if the new term improves the model more than would be expected by chance. It decreases when a predictor improves the model by less than expected by chance. Normally the adjusted R-square is lower than R-square [24]. The standard error of the estimate (SEE) is a measure of the accuracy of predictions. Recall that the regression line is the line that minimizes the sum of squared deviations of prediction (also called the sum of squares error). The standard error of the estimate is closely related to this quantity and is defined as:

$$SEE = \sqrt{\frac{\sum(Y-Y')^2}{N}} \qquad (1)$$

Where Y is an actual score, Y' is a predicted score, and N is the number of pairs of scores. The SEE for the nitrided layer below surface and duration of nitriding time is 0.1512. In a scatterplot in which the SEE is small, one would therefore expect to see that most of the observed values cluster fairly closely to the regression line. When the SEE is large, one would expect to see many of the observed values far away from the regression line which means the model with the smallest standard error of estimate (SEE) is the best fit for the sample [25].

The equation obtained from the curve fitting by using Sigma Plot software is

$$F=1.9491(1-0.7947X) \qquad (2)$$

Where F is nitrided layer thickness, and X is duration of nitriding time. The curve obtained is the best fit graph when the value of R^2 recorded is 0.9709 which is the values close to 1 indicates a good fit. Besides that, the value of Standard Error of Estimate (SEE) obtained also show the best fit for the sample when value recorded is 0.1512 which is the smallest value achieved by the curve-fitting.

3.4 Effective Duration of Nitriding

Equation 2 is extrapolated until 48 hours. The depth of nitrogen penetration in AISI 316L nitrogenized at 1200°C can be obtained by case depth method and it shown in the Figure 5. From the graph, the rate of diffusion of nitrogen into the samples is increasing rapidly from 0 to 5 hours.

However, it slow down after 5 hours and when the duration of gas nitriding process approaches 18 hours, the depth of nitrogen penetration below the surface is remains constant at 1.9 mm, even if the duration of nitriding process increases. Hence, there is no point to extend the gas nitriding process by using same parameter to achieve higher thickness of nitrided layer.

4 Conclusions

The nitrided AISI 316L have better surface hardness compare to the as-received samples. The microhardness at the surface of the nitrided sample achieved is 345HV which is increases by 58%. Besides that, the grain size of the microstructure tends to be enlarged when nitriding time increases and formation of twins were observed. Based on the experimental result of the hardness value at 245HV, the equation of effective duration of gas nitriding process was formed by using the Sigma Plot software, so that the duration of gas nitriding process can be estimated to obtain a desired thickness of nitrided layer.

Acknowledgement

The authors would like to thank University Technology PETRONAS and Ministry of Higher education Malaysia for funding this research work under FRGS.

References

1. From *http://sppusa.com/reference/stainless_steel/steel.html* (2013)
2. T. Kumar, P. Jambulingam, M. Gopal and A. Rajadurai, *ISRS 2004-04* (2004)
3. ASM International, "*Stainless Steel for Design Engineers*", American Technical Publishers Ltd. Chap. **6** (2008)
4. J. R. Davis, "*Surface Hardening of Steel*", ASM International, pp.141-194, (2002).
5. ASM International, "*Practical Nitriding and Ferritic Nitrocarburizing*", American Technical Publishers Ltd. Chap. **1**, (2003)
6. D.Q. Peng, T.H. Kim, J.H. Chung, J.K. Park, ASC., **256**, no.24, pp.7522-7529, (2010)
7. P. Kochmański and J. Nowacki, Surface & C.T. **202**, pp. 4834-4838, (2008)
8. L. Wang, S. Ji, J. Sun, Surface & C.T., **200,** pp. 5067–5070, (2006)
9. S.M. Hassani-Gangaraj and M. Guagliano, ASC., **271**, pp. 156–163, (2013)
10. F.C. Campbell, ASM International, Chap. **21**, (2008)
11. J. D. Kamminga & G. C. A. M. Janssen, Surface & C.T. **200** 5896–5901,(2006)
12. S. Mridha & A. A. Khan, MPT. **201**, Pages 325–330 (2008)
13. E. Menthe & K. T. Surface & C.T. **116–119**, Pages 199–204, (1999)
14. H. Firmanto, P. Hussain & O. Mamat, *J. of Applied Sciences* **11***: 1809-1814*, (2011)
15. D. C. Zipperian, *Metallographic Specimen Preparation Basics*, www.metallographic.com
16. J. F. Shackelford, *Introduction to Materials Science for Engineers* 7th ed., (2009)
17. S. Vercammen, Acta Materialia **52**, Issue 7, pp. 2005–2012, (2004)
18. R.-b. Song, J.-y. Xiang, D.-p. Hou, J. of I.&S.R. **18**, Issue 11, pp. 53–59, (2011)
19. D. H. Herring, *The Heat Treat Doctor*, Industrial Heating, (2005)
20. P. Hussain, *Diffusion Bondaing of Sailon and Stainless Steel* (1997)
21. J. F. Santos, C. M. Garzón, A. P. Tschiptschin, M.S.& E. A **382** pp.378–386 (2004)
22. Feder, A., Alcala, J., Llanes L., Anglada, M, J. of T.E.C.S. **23**, pp. 2955-2962(8) (2003)
23. J. V. Gurley, "*Numerical Method: Curve Fitting Technique*", (1992)
24. J. Frost: http://blog.minitab.com/, (2013)
25. M. L. McHugh, Retrieved from http://www.biochemia-medica.com, (2007)